Formation Mechanism of Needle-like α-Fe$_2$O$_3$ Particles Grown Along the c Axis and Characterization of Precursorily Formed β-Fe$_2$O$_3$

Yasunori IKEDA*, Mikio TAKANO* and Yoshichika BANDO*

The formation mechanism of needle-like α-Fe$_2$O$_3$ particles prepared by calcination of a mixture of iron (III) sulphate and sodium chloride was studied through X-ray diffraction, SEM and TEM measurements. These particles are grown along the c axis. The reaction process was found to include the following important steps:

$$3NaFe(SO_4)_2 \longrightarrow Na_3Fe(SO_4)_3 + \beta\text{-}Fe_2O_3 + 3SO_3$$
$$2Na_3Fe(SO_4)_3 + 2\beta\text{-}Fe_2O_3 \rightarrow 3\alpha\text{-}Fe_2O_3 + 3Na_2SO_4 + 3SO_3$$
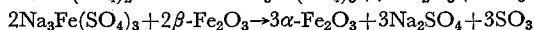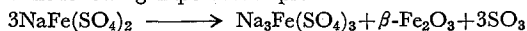
The precursorily formed β-Fe$_2$O$_3$ particles could be isolated for characterization by X-ray diffraction, SEM, TEM, magnetic measurement, and Mössbauer spectroscopy. This material is isostructural with bixbyite and the lattice constant is $a_0 = 9.398$ Å. As for the magnetism, it is an antiferromagnet with a Nèel temperature of 119 K.

INTRODUCTION

α-Fe$_2$O$_3$ particles with various morphologies have been used widely as a raw material for preparation of γ-Fe$_2$O$_3$, a useful magnetic recording material, and other ferrites. The morphological control has been studied by many researchers. Matijević et al., for example, obtained particles with various shapes such as cube, sphere, and spindle by forced hydrolysis of acidified ferric salt solutions at elevated temperatures[1,2,3]. But the orientation of the crystalline axes within those particles has not been reported except for the case of the cubic particles. Tallman and Gulbrasen reported the morphology and growth mechanism of α-Fe$_2$O$_3$ whiskers, which are blade-like platelets, formed on metallic iron at 400~500°C in dry oxygen[4,5]. They concluded that the platelets consisted of twinned crystals and that the blade axis and the blade face plane were [$\bar{1}\bar{1}$20] and ($\bar{1}$101), respectively. We have reported that needle-like particles with the hexagonal c axis along the longitudinal direction could be obtained by calcination of a mixture of iron (III) sulfate, Fe$_2$(SO$_4$)$_3$, and an alkaline salt such as sodium chloride and sodium sulphate[6]. To our knowledge, this is the only study reporting the formation of needle-like α-Fe$_2$O$_3$ particles grown along the c axis. This paper will outline the formation mechanism. We have been keenly interested in the mechanism, because the formation of elongated hexagonal prisms is contradictory to the common sense that

* 池田靖訓, 高野幹夫, 坂東尚周 : Laboratory of Solid State Chemistry, Institute for Chemical Research, Kyoto University, Uji, Kyoto 611.

the closed packed c plane tends to grow.

It is very characteristic that β-Fe_2O_3 has been found to appear intermediately in the reaction process. There are three polymorphs, α-, β-, and γ-forms, of Fe_2O_3 among which α- and γ-Fe_2O_3 have already been well-known. However, there have been very few reports about β-Fe_2O_3. Bonnevie-Svendsen was the first to announce the existence of β-Fe_2O_3, which was prepared by hydrolysis of $FeCl_3 \cdot 6H_2O$[7]. Cubic structure with a lattice constant of $a_0 = 9.40$ Å was assigned. Geller et al.[8] and Grant et al.[9] 'predict'ed the existence of a cubic polyform from crystallographic considerations on the In_2O_3-Fe_2O_3 and Sc_2O_3-Fe_2O_3 systems. Lina Ben-Dor et al.[10,11] reported chemical vapour deposition of β-Fe_2O_3 films consisting of fine particles ($\sim$500 Å) from iron trifluoroacetylacetone at 300°C onto various substrates. The films were characterized by X-ray diffraction (XRD), SEM and Mössbauer spectroscopy. However, the films were found to be contaminated with a large amount of α-Fe_2O_3. We successfully isolated pure and bulky particles ($\approx$1 μm) of β-Fe_2O_3. In this paper, we report some magnetic properties and the role of this material in the formation process of the α-Fe_2O_3 particles with the unique morphology.

EXPERIMENTAL

The starting materials were $Fe_2(SO_4)_3$ and NaCl of the reagent grade. These were thoroughly mixed in an agate mortar with various ratios. The mixtures were placed on Al_2O_3 trays and calcined in the air under various conditions with respect to temperature and time. After cooling to room temperature, the reaction products were dispersed in distilled water, filtered, and washed with distilled water. Phase identification and determination of lattice parameters were carried out by means of powder X-ray diffraction using graphite-monochromated $CuK\alpha$ radiation. The diffractometer was Rigaku RU-200. Si (99.999%) powder was used as an internal standard when necessary. The measurement was extended to 1073 K using a platinum furnace. Magnetic properties of β-Fe_2O_3 were measured with a SQUID magnetometer (SHE) between 4.2 K and 300 K. The Mössbauer effect (ME) was measured in the same temperature range using a $^{57}Co/Rh$ source. Metallic iron was used as a control sample for velocity calibration and as the isomer shift reference. Identification of crystalline phases, observation of the particle shape and size were carried out by means of TEM (JEOL-7A) and SEM (JEOL-200T). TG-DTA measurements were made between 300 K and 1073 K in the air using an apparatus of Rigaku TG4-DT6.

RESULTS AND DISCUSSION

I. Formation Mechanism of Needle-like α-Fe_2O_3 Particles —Part 1

When a mixture of $Fe_2(SO_4)_3$ and NaCl was heated in the air above 700°C, the final product was always a mixture of α-Fe_2O_3 and Na_2SO_4. However, as reported in our previous paper[6], the morphology of the α-Fe_2O_3 particles depended on the composition of the starting mixture, heating temperature, and time; the composition, especially, had a crucial effect. Needle-like particles with a length

of 1~15 μm and a width of ~1 μm could be obtained uniformly by calcination of the mixture with a molar ratio of Fe$_2$(SO$_4$)$_3$: NaCl=1:2 at 700°C for 1 hr. Typical SEM and TEM micrographs of these particles are given in Fig. 1 (A) and (B). Both the top and lateral planes of the hexagonal prisms are smooth, without steps or cracks, at the magnification used by us. Electron diffraction patterns and the corresponding dark field images showed the longitudinal direction to be [0001].
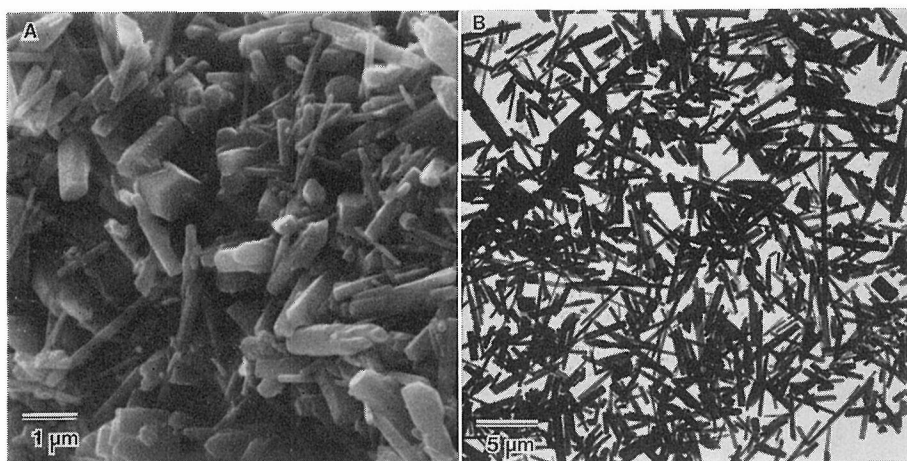

Fig. 1. SEM (A) and TEM (B) micrographs of needle-like α-Fe$_2$O$_3$ particles.

The reaction process was studied by calcining the starting mixtures at lower temperatures for 1 h to slow down the reaction rate. Summarized in Table 1 are the intermediate compounds identified by XRD obtained from the 1:2 starting mixture. These results suggested that the reaction process consisted of the following three important stages.
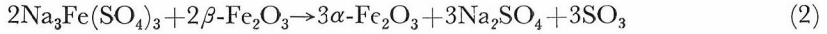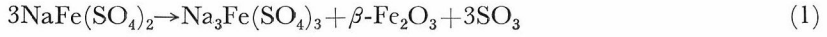
Table I. Compounds identified by XRD contained in the products obtained by calcination of the mixture with a molar ratio of Fe$_2$(SO$_4$)$_3$: NaCl=1: 2 at various temperatures for 1 hr in the air.

Compound	Calcination Temperature (°C)									
	200	300	400	500	575	600	625	650	675	700
NaCl	○	○	○							
Fe$_2$(SO$_4$)$_3$	○	○	○	○						
NaFe(SO$_4$)$_2$	○	○	○	○	○	○				
Na$_3$Fe(SO$_4$)$_3$			○	○	○	○	○			
Na$_2$SO$_4$								○	○	○
β-Fe$_2$O$_3$				○	○	○	○	○		
α-Fe$_2$O$_3$						○	○	○	○	○

1) At the first stage, NaFe(SO$_4$)$_2$ was produced by reaction of Fe$_2$(SO$_4$)$_3$ and NaCl.
2) At the second stage, NaFe(SO$_4$)$_2$ was decomposed gradually to β-Fe$_2$O$_3$ and Na$_3$Fe(SO$_4$)$_3$.

3) At the last stage, α-Fe_2O_3 and Na_2SO_4 were produced by reaction of $Na_3Fe(SO_4)_3$ and β-Fe_2O_3.

Though the reaction at the first stage remains somewhat unresolved, the second and the third stages may be expressed by the following equations.

$$3NaFe(SO_4)_2 \rightarrow Na_3Fe(SO_4)_3 + \beta\text{-}Fe_2O_3 + 3SO_3 \tag{1}$$

$$2Na_3Fe(SO_4)_3 + 2\beta\text{-}Fe_2O_3 \rightarrow 3\alpha\text{-}Fe_2O_3 + 3Na_2SO_4 + 3SO_3 \tag{2}$$

The precursory formation of β-Fe_2O_3 has been found to be essentially important for the formation of needle-like α-Fe_2O_3 particles as will be described later.

II Formation Process and Characterization of β-Fe_2O_3

A SEM photograph of the product obtained by calcination of the 1:2 mixture at 550°C for 1 hr is shown in Fig. 2. Cubic particles like the one indicated by an arrow correspond to β-Fe_2O_3. According to XRD, the product contained two
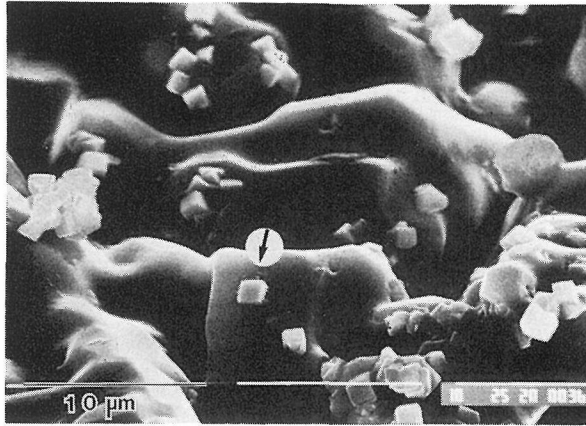

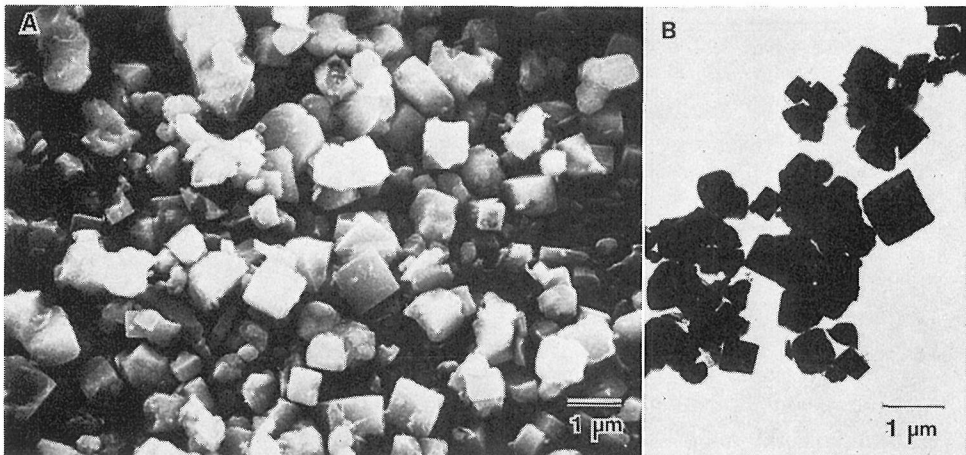Fig. 2. A SEM micrograph of the product obtained by calcination of the 1:2 mixture at 550°C for 1 hr. An arrow point to a β-Fe_2O_3 particle.

Fig. 3. SEM (A) and TEM (B) micrographs of isolated β-Fe_2O_3 particles.

other phases which were NaFe(SO$_4$)$_2$ and Na$_3$Fe(SO$_4$)$_3$. However, the two latter phases could be identified in the photograph only as a homogenous bulk with a wavy smooth surface like that of a quenched liquid. Figure 3 shows SEM (A) and TEM (B) micrographs of the β-Fe$_2$O$_3$ particles isolated by washing with distilled water.

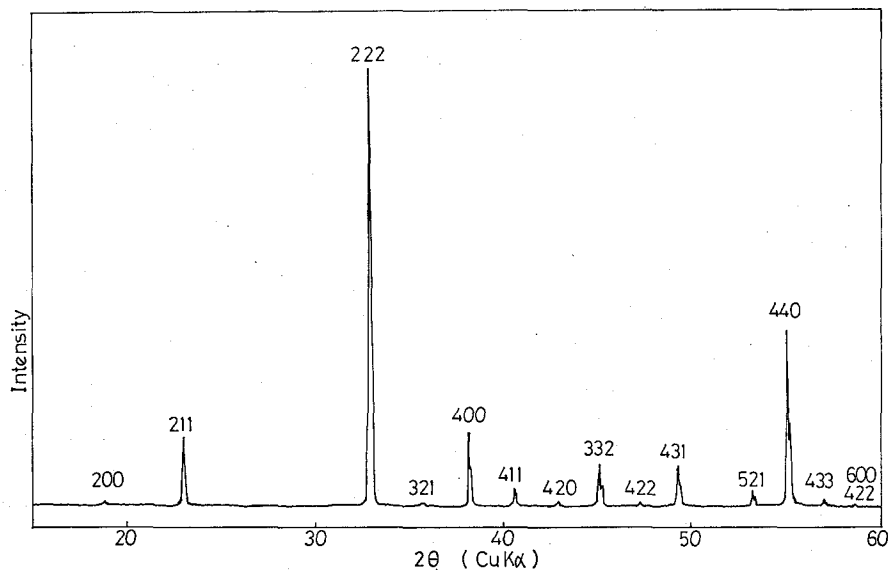The XRD pattern obtained is shown in Fig. 4. All the diffraction peaks were

Fig. 4. XRD pattern of β-Fe$_2$O$_3$.

very sharp and could be assigned to the bixbyite-type structure with space group Ia3[7]. The cell dimension was determined to be a$_0$=9.398±0.001 Å. The XRD data are summarized in Table 2. It should be emphasized here that any diffraction peak assignable to α-Fe$_2$O$_3$ could not be detected at all even by a very carefull measurement. Electron diffraction measurements confirmed that each particle was a single crystal. It should be noted in Fig. 3 that β-Fe$_2$O$_3$ tends to form cubic particles with the {100} facets. However, the shape is not perfect, some corners being apparently torn off. We have supposed that this results from the following growth mechanism. β-Fe$_2$O$_3$ nucleates on thermal decomposition of NaFe(SO$_4$)$_2$, when Na$_3$Fe(SO$_4$)$_3$, which is simultaneously formed, and residual NaFe(SO$_4$)$_2$ produce a eutectic liquid phase around the nuclei. The eutectic nature was suggested not only from Fig. 2 but also from the fact that pure Na$_3$Fe(SO$_4$)$_3$ remains solid at 550°C as found by our independent experiment. Elements necessary for the growth of the nuclei are supplied from NaFe(SO$_4$)$_2$ through the liquid.

DTA and XRD measurements at elevated temperatures showed that β-Fe$_2$O$_3$ began to be transformed to α-Fe$_2$O$_3$ at about 600°C. The transformation was gradual but was accelerated at higher temperatures. It finished within a few minutes at 780°C. The α-Fe$_2$O$_3$ particles were also single-crystalline cubic particles. Topotactic relations between these polymorphs are under examination.

Table II.　List of the X-ray data of β-Fe_2O_3 crystallizing in the cubic
bixbyite structure; a_0=9.398 Å.

d (obs.)	d (cal.)	(I/Io)	(H K L)
4.70	4.70	<1	(200)
3.838	3.837	15	(211)
2.714	2.713	100	(222)
2.513	2.512	1	(321)
2.350	2.350	16	(400)
2.216	2.215	5	(411)
2.102	2.101	1	(420)
2.005	2.004	10	(332)
1.919	1.918	1	(422)
1.844	1.843	9	(431)
1.717	1.716	4	(521)
1.662	1.661	40	(440)
1.612	1.612	2	(433)
1.567	1.566	<1	(600), (442)
1.525	1.525	5	(611), (532)
1.487	1.486	1	(620)
1.451	1.450	4	(541)
1.417	1.417	19	(622)
1.387	1.386	5	(631)
1.357	1.356	3	(444)
1.330	1.329	1	(543)
1.304	1.303	1	(640)
1.280	1.279	3	(721), (633), (552)
1.257	1.256	1	(642)
1.194	1.194	1	(732), (651)
1.176	1.175	3	(800)
1.158	1.157	2	(811), (741), (554)
1.141	1.140	1	(820), (644)
1.124	1.123	1	(653)
1.108	1.108	1	(822), (660)
1.093	1.093	2	(831), (743)
1.079	1.078	4	(662)
1.051	1.051	2	(840)
1.038	1.038	<1	(833)
1.026	1.025	<1	(842)
1.014	1.013	1	(921), (761), (655)
1.002	1.002	<1	(664)
.991	.991	1	(851), (754)
.970	.969	1	(932), (763)
.959	.959	3	(844)
.950	.949	1	(941), (853)
.940	.940	1	(860)
.931	.931	<1	(772)
.922	.922	2	(862)
.913	.913	<1	(943)
.905	.904	2	(666)
.896	.896	2	(952), (765)

Temperature dependences of the magnetic susceptibility, χ, and the inverse susceptibility, χ^{-1}, are shown in Fig. 5. Field dependence of the magnetization at 4.2 K is also shown in Fig. 6. These data clearly indicate that β-Fe$_2$O$_3$ is an
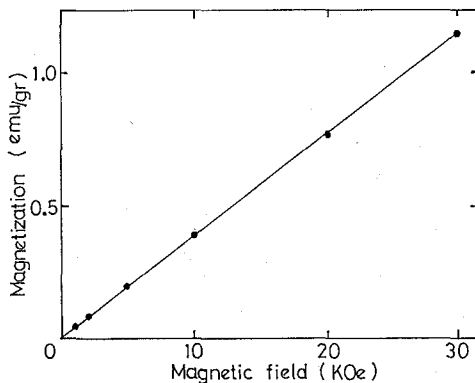
Fig. 6. Magnetic field dependence of the magnetization of β-Fe$_2$O$_3$ at 4.2 K.
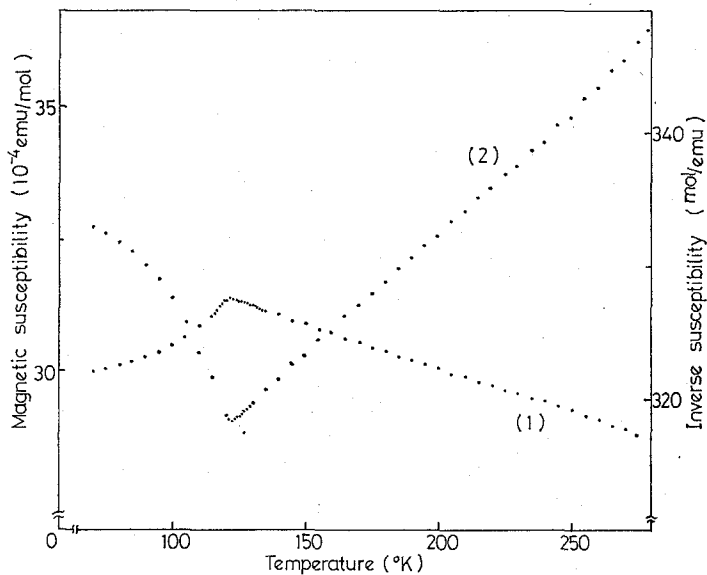
Fig. 5. Temperature dependence of the magnetic susceptibility (1) and its inverse (2) of β-Fe$_2$O$_3$ at 5kOe.

antiferromagnetic substance with a Nèel temperature of 119 K. The asymptotic Nèel temperature and the effective Bohr magneton number were derived from the Curie-Weiss law holding in the paramagnetic state. The former was −1635 K and suggested a very strong antiferromagnetic exchange interaction between the Fe^{3+} ions. The latter was 6.64, which was slightly larger than the expected spin-only value of 5.92 for a Fe^{3+} ion in high spin state. However, similar values of 6.4 and −2940 K were reported also for α-Fe$_2$O$_3$[12]. As the cation sites in the bix-byite structure form an approximately face-centered-cubic lattice which does not

allow a simple collinear antiferromagnetic spin structure, a neutron diffraction study is of great interest and is in progress. Figure 7 shows the ME spectra at 300 K and 4.2 K. The spectrum at 300 K looks like a single quadrupole doublet with an isomer shift of 0.38 mm/s and a quadrupole splitting of 0.75 mm/s, though there
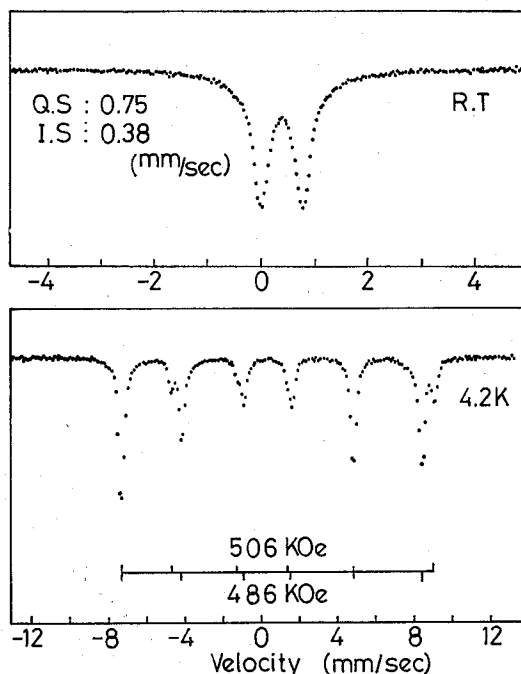

Fig. 7. ME spectra of β-Fe_2O_3 at 300 K and 4.2 K.

are two kinds of cation sites, 24 d and 8 b, with a relative abundance of 3:1. However at 4.2 K, two sets of magnetic hyperfine patterns with hyperfine fields of 506 kOe and 486 kOe can be seen, and the relative intensity is near 3:1. Measurements at intermediate temperatures confirmed the antiferromagnetic transition at 119 K. The spectra at low temperatures are useful in elucidating the spin structure. Further details will be reported elsewhere together with the results of the neutron diffraction measurements.

III Formation Mechanism of Needle-like α-Fe_2O_3 Particles—Part 2

In this section we shall show the key role of β-Fe_2O_3 in the formation process of the needle-like α-Fe_2O_3 particles, and a probable formation mechanism will be discussed in brief. It is interesting to study the reaction of well-characterized β-Fe_2O_3 and $Na_3Fe(SO_4)_3$ particles. Single phase β-Fe_2O_3 particles, isolated as described in the preceding section, and $Na_3Fe(SO_4)_3$, prepared by condensation of an aqueous solution containing Na_2SO_4 and $Fe_2(SO_4)_3$ in a molar ratio of 3:1, were thoroughly mixed in a molar ratio of 1:1 as given in eq. (2) and heated on an alumina tray at 700°C for 1 h in the air. The product was a mixture of α-Fe_2O_3 and Na_2SO_4 as found by XRD. A SEM observation of the α-Fe_2O_3 particles isolated
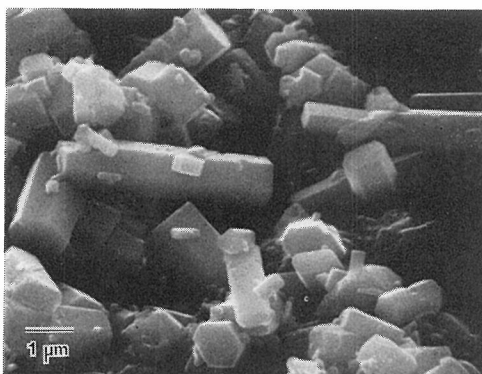
Fig. 8. A SEM micrograph of α-Fe$_2$O$_3$ obtained by calcination of the mixture with a molar ratio of β-Fe$_2$O$_3$: Na$_3$Fe(SO$_4$)$_3$=1:1 at 700°C for 1 hr in the air.

by washing with distilled water is shown in Fig. 8. It could be clearly seen that thick hexagonal prisms of α-Fe$_2$O$_3$ were formed from the mixture, though a similar heat treatment of each constituent alone never produced such particles. It is interesting to point out here that the area of a hexagonal top plane is, generally, similar to that of the (100) or (110) plane of an original β-Fe$_2$O$_3$ particle.

From various experimental results including those mentioned above, we can at least mention the following important steps in the formation of beautiful hexagonal-prismatic α-Fe$_2$O$_3$ particles. β-Fe$_2$O$_3$ seems to be dissolved into and precipitated as α-Fe$_2$O$_3$ from molten Na$_3$Fe(SO$_4$)$_3$ (m.p. $\approx$600°C). The dissolution does not extend deep into a particle of β-Fe$_2$O$_3$ before α-Fe$_2$O$_3$ precipitates on it epitaxially. The inner part can be automatically transformed into α-Fe$_2$O$_3$ which is stabler at 700°C. Elements necessary for the particle growth are supplied from Na$_3$Fe(SO$_4$)$_3$. The decomposition of this sulfate seems to be promoted by the presence of either α- or β-Fe$_2$O$_3$: the liquid sulfate can remain stable when alone as found by an independent experiment. The participation of molten Na$_3$Fe(SO$_4$)$_3$ gives rise to the well-defined crystal habit.

ACKNOWLEDGEMENTS

REFERENCES

(1) S. Hamada and E. Matijević, *J. Colloid Interface Sci.*, **84**, 274 (1981)
(2) E. Matijević and P. Scheiner, *ibid.*, **63**, 509 (1978)
(3) M. Ozaki, S. Kratohvil and E. Matijević, *ibid.*, **102**, 146 (1984)
(4) R.L. Tallman and E.A. Gulbransen, *J. Electrochem. Soc.*, **114**, No. 12, 1227 (1967)
(5) R.L. Tallman and E.A. Gulbransen, *ibid.*, **115**, No. 7, 770 (1968)
(6) Y. Bando, Y. Ikeda and K. Okuda, *Rep. Asahi Glass Found. Ind. Technol.*, **43**, 199 (1983)
(7) M. Bonnevie-Svendsen, *Naturwissenschaften.*, **45**, 542, (1958)

(8) S. Geller, H.J. Williams and R.C. Sherwood, *J. Chem. Phys.*, **35**, 1908 (1968)

(9) R.W. Grant, S. Geller, J.A. Cape and G.P. Espinoza, *Phys. Rev.*, **175**, 686 (1968)

(10) L. Ben-Dor and E. Fischbein, *Acta Cryst.*, **B32**, 667 (1976)

(11) L. Ben-Dor, E. Fischbein, I. Felner and Z. Kalman, *J. Electrochem. Soc.*, **124**, No. 3, 451 (1977)

(12) L. Néel and R. Pauthenet, *Compt. Rend.*, **234**, 2172 (1952)